DOI: 10.31401/WS.2024.proc.12

An Assessment of the Radiation Risk in Orbit Around Mars, Based on Measurements by the Lyulin Instrument and Numerical Simulations

Krastev K.[1], Semkova J.[1], Koleva R.[1], Benghin V.[2], Drobyshev S.[2]

[1]Space Research and Technology Institute, Bulgarian Academy of Sciences
[2] Institute of Biomedical Problems of Russian Academy of Sciences

Abstract

In this paper, we present the results of the numerical modeling of the Liulin device. Some effects that occur when ionizing radiation is detected by a system of detectors (telescope) are described.

Introduction

The issues and methodology discussed in this article follow those presented in [Krastev et all., 2023a]. Here we will focus on the influence of the geometry of the detectors and the design of the Liulin - MO device on the measured fluxes and doses. The Lyulin-MO dosimetry module of the FREND instrument provides information on the radiation environment during the cruise stage and in orbit around Mars [Semkova et al, 2018]. A schematic diagram of the construction and geometry of the instrument's detectors is shown in Figure 1.

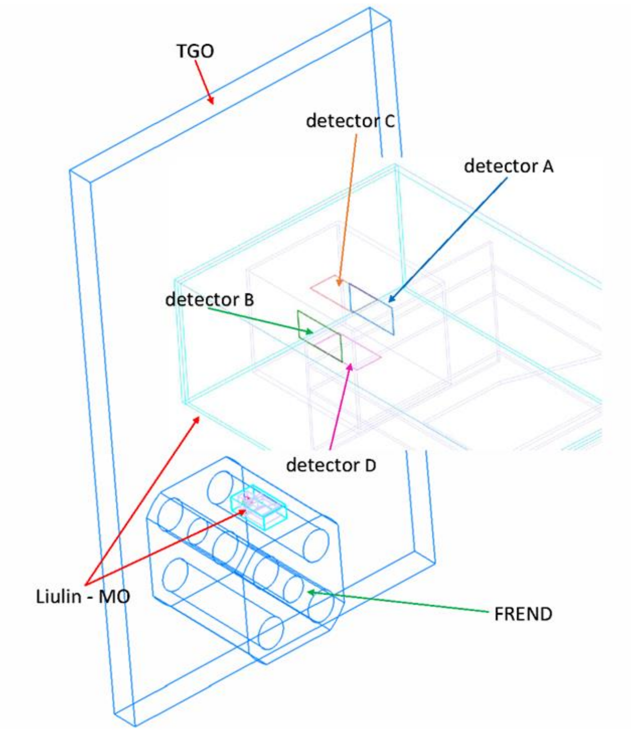

Figure 1. *The detector circuit of the Lyulin-MO equipment on board TGO.*

One of the significant effects affecting the accuracy of measurements is shown in Figure 2.

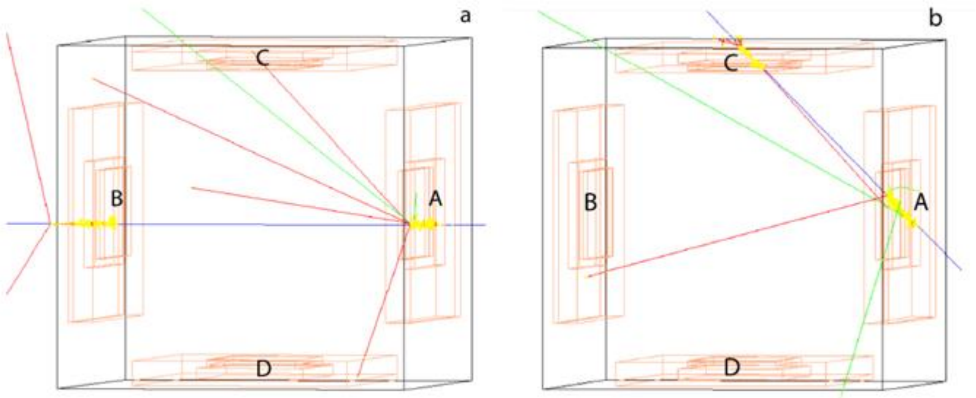

Figure 2. *Examples of true and false signals: a) A heavy particle (shown in blue) passes through each of the detectors A and B included in the telescope AB. This is an example of a real coincidence. Here, a parasitic signal is generated by a DC telescope. Detectors D and C register secondary electrons in the matching mode and give a false match; b) A heavy particle (blue color) passes through only one of the detectors (detector A), a coincidence is recorded caused by the ingress of secondary particles (red color) into detector B. In this case, we have a false match.*

Methods

The methodology for research and evaluation of the specified effects follows that described in [Krastev et all., 2023]. The corresponding distribution for the GCR flux is taken from the NASA OLTARIS database (https://oltaris.larc.nasa.gov/), Figure 3. The GCR model of Badhwar O'Neil (BON 2020) [Slaba & Withman, 2020] is used. Data used for the period from April 15, 2016 to September 15, 2016.

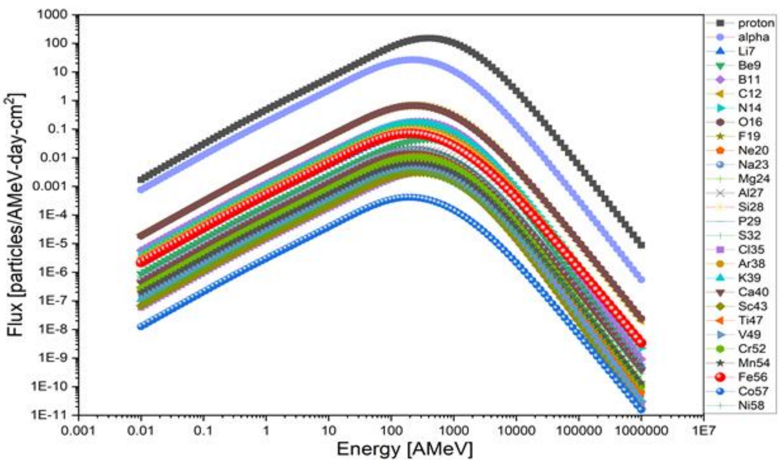

Figure 3. *Spectrum of galactic cosmic rays GCR from NASA's OLTARIS database*

Results

Figure 4 shows for each component of the GCR spectrum in which energy range it is registered. It can be seen from the figure that heavy elements, due to the effects shown in Figure 2, are registered in a lower energy range than they should be. This effect has a minor role in the formation of the flux since it is overshadowed by the recorded protons and alpha particles whose count rate is orders of magnitude higher. In the considered case of protection, the highest energy part of the spectrum is formed by registration of iron ions, but Mg24 and Si28 ions have a significant contribution.

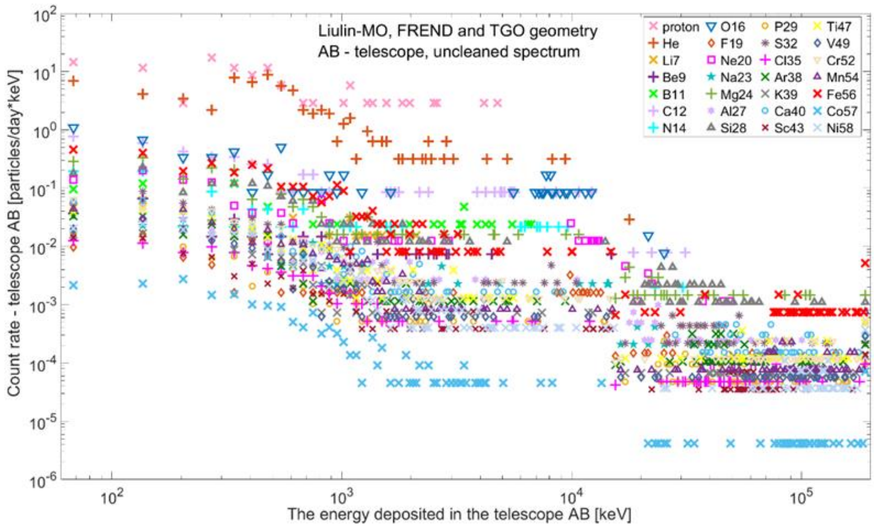

Figure 4. *Count rate (uncleared) of the AB telescope, for each component of the GCR, calculated from the simulation. The protection includes Lyulin-MO, FREND and TG*

Figure 5 shows how the readings of the detector system depend on the surrounding structures and materials. For a more precise analysis, the geometric factors are calculated separately for detectors A and B, denoted by GA and GB, respectively. From Figure 5 it can be seen that the geometric factor GB for the high-energy range obtained in the case of shielding is 35 cm^2 sr, and this same GB factor in the case of zero shielding is 1.4 cm^2 sr. It can be said that the role of electrons in event registration increases sharply in the case of protection of the detector system. On the contrary, in the high-energy range, the geometric factor in the case of shielding is smaller than that for zero shielding. This can be explained by the shielding of part of the GCR flux by the construction of Lyulin-MO, FREND and TGO.

Figure 6 shows the cleaned spectra for the AB telescope. It can be seen from the figure that only protons and alpha particles are present in the lowest energy range. It can also be noted that the cleaned spectra lack the "tails" of most of the components, i.e. the events in which the recorded energy goes beyond the scope of the telescope (192 MeV). Here, by a cleaned spectrum, we will understand a simulated spectrum from which parasitic signals are removed.

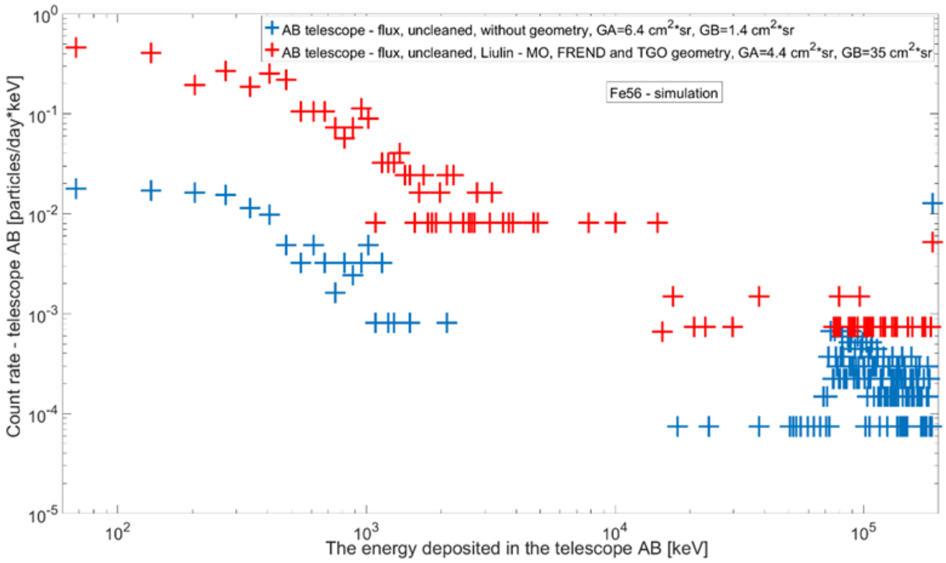

Figure 5. *Count rate (uncleared) of the AB telescope, for Fe56 from the GCL spectrum, calculated from the simulation for the cases without shielding and with shielding by the construction. Protectione includes Liulin-MO, FREND and TGO.*

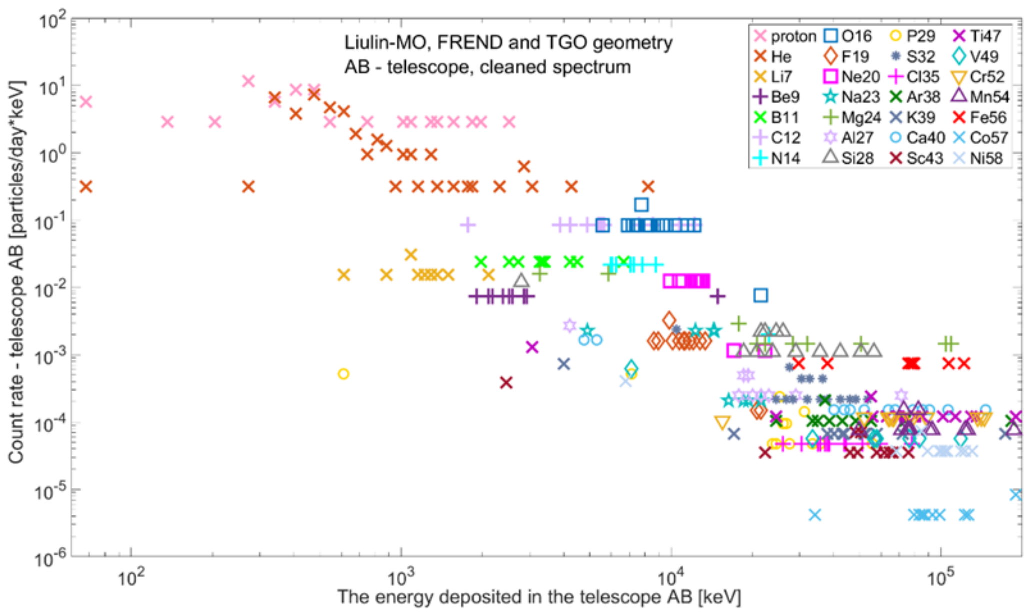

Figure 6. *Count rate (cleared) of the AB telescope, for each component of the GCR, calculated from the simulation. protection includes Lyulin-MO, FREND and TGO.*

Conclusion

The obtained numerical simulation results show that the registration of ionizing radiation by detector systems (telescopes) is accompanied by the appearance of undesirable effects that distort the detector response. Failure to take these effects into account in some cases leads to overestimation of measurements by several times. The use of false signal cleaning methods [Krastev et all., 2023b], which are not considered here, leads to results close to those obtained experimentally [Semkova, J., et al, 2018; Zeitlin, C., et al. 2013].

References

Krastev K., et al 2023a. Numerical Simulation of the LIULIN-MO Device, pp.88-94, Proceedings of the 15th Workshop "Solar Influences on the Magnetosphere, Ionosphere and Atmosphere" June, 2023, ISSN 2367-7570, pp.88-94, https://spaceclimate.bas.bg/ws-sozopol/pdf/Proceedings2023.pdf

Krastev, K. et al, 2023b, Numerical simulation of Liulin-MO instrument for measuring cosmic radiation onboard Exomars Trace Gas Orbiter, Comptes rendus de l'Académie bulgare des Sciences, Tome 76, No , 2023

Semkova, J., et al, 2018. Charged particles radiation measurements with Liulin-MO dosimeter of FREND instrument aboard ExoMars Trace Gas Orbiter during the transit and in high elliptic Mars orbit, Icarus, Vol. 303, Pp 53-66, https://doi.org/10.1016/j.icarus.2017.12.034

Slaba T. & K. Withman, „The Badhwar-O'Neill 2020 GCR Model", AGU, Volume18, Issue 6, 2020

Zeitlin, C., et al. 2013. Measurements of Energetic Particle Radiation in Transit to Mars on the Mars Science Laboratory, Science 340, 1080 (2013)